International Journal of Geographical Information Science
Vol. 20, No. 2, February 2006, 169–192

Taylor & Francis
Taylor & Francis Group

Research Article

The accuracy of grid digital elevation models linearly constructed from scattered sample data

FERNANDO J. AGUILAR*, MANUEL A. AGUILAR, FRANCISCO AGÜERA and JAIME SÁNCHEZ

Department of Agricultural Engineering, University of Almeria, Spain, Ctra. de Sacramento s/n. La Cañada de San Urbano, 04120 Almería, Spain

(*Received 28 March 2005; in final form 7 September 2005*)

In this paper, a theoretical-empirical model is developed for modelling the accuracy of a grid digital elevation model (DEM) linearly constructed from scattered sample data. The theoretical component integrates sample data accuracy in the model by means of the error-propagation theory. The empirical component seeks to model what is known as information loss, i.e. the sum of the error due purely to sampling the continuous terrain surface with a finite grid interval and the interpolation error. For this purpose, randomly spaced data points, supposed to be free of error, were converted into regularly gridded data points using triangulation with linear interpolation. Original sample data were collected with a 2×2 m sampling interval from eight different morphologies, from flat terrain to highly rugged terrain, applying digital photogrammetric methods to large-scale aerial stereo imagery (1 : 5000). The DEM root mean square error was calculated by the true validation method over several sets of check points, obtaining the different sampling densities tested in this work. Several empirical models are calibrated and validated with the experimental data set by modelling the DEM accuracy by combining two variables such as sampling density and a descriptive attribute of terrain morphology. These empirical models presented a morphology based on the product of two potential functions, one related to the terrain roughness and another related to the sampling density. The terrain descriptors tested were average terrain slope, standard deviation of terrain slope, standard deviation of unitary vectors perpendicular to the topographic surface (SDUV), standard deviation of the difference in height between adjacent samples in the grid DEM (SDHD), and roughness estimation by first-, second-, or third-degree surface fitting error. The values obtained for those terrain descriptors were reasonably independent from the number and spatial distribution of the sample data. The models based on descriptors SDHD, SDUV, and standard deviation of slope provided a good fitting to the data observed ($R^2 > 0.94$) in the calibration phase, model SDHD being the one that yielded the best results in validation. Therefore, it would be possible to establish *a priori* the optimum grid size required to generate or store a DEM of a particular accuracy, with the saving in computing time and file size that this would mean for the digital flow of the mapping information in GIS.

Keywords: Grid digital elevation models; Interpolation; Quality assessment of spatial data; Digital elevation model accuracy; Modelling

*Corresponding author. Email: faguilar@ual.es

International Journal of Geographical Information Science
ISSN 1365-8816 print/ISSN 1362-3087 online © 2006 Taylor & Francis
http://www.tandf.co.uk/journals
DOI: 10.1080/13658810500399670

1. Introduction

Digital elevation models (DEMs) have become one of the most important covers for Geographical Information Systems (GIS) in many disciplines, which highlight the need to assess DEM accuracy. If GIS users are not aware of the DEM accuracy, perfectly logical GIS analysis techniques can lead to incorrect results. In other words, the data may not be fit for use in a certain context (Fisher 1998).

The awareness of the GIS user community of this problem is shown by the vast number of studies published in the last few years on error detection, both quantitative methods based on statistical-mathematical algorithms (e.g. Felicísimo 1994, López 1997, Briese *et al.* 2002) and qualitative methods based on visualization techniques (Wood and Fisher 1993, Wood 1996, Yang and Hodler 2000).

It must be borne in mind that the DEM data-acquisition phase has reached a remarkable degree of development with the introduction of new technologies, such as the laser scanner (LIDAR) and InSAR (Smith 2004), which allow a high degree of automation and density sensing. Thus, the US Geological Survey scientists are now finding new methods for the use and representation of high-resolution LIDAR data (Queija *et al.* 2005). Therefore, the problem nowadays is not obtaining data from a DEM, but handling and maintaining such an amount of information using structures, which will allow its efficient integration and exploitation in GIS or CAD areas. In the majority of cases, it is preferable to have an optimized DEM adapted to our needs, i.e. without excess information, rather than to have a vast amount of data, which will be more difficult for us to handle (Aguilar *et al.* 2005). Thus, optimum sampling strategies are clear favourites to guarantee the quality requirements of a DEM with the lowest possible number of points (Balce 1987).

It seems obvious that the user and the producer of DEMs need to agree on the accuracy and the grid interval of the product, among other specifications (Huang 2000). To this end, they should speak the same language and have models at their disposal that will allow them to predict the grid DEM accuracy in terms of the main factors that intervene in its definition: accuracy and density of the data source, characteristics of the terrain surface and the method used for the construction of the DEM surface (Li 1992, Gong *et al.* 2000). The work presented in this paper is focused on this last point.

Most of the models developed in the last few years for modelling the global error of a DEM can be classified as empirical or theoretical. Within the empirical models, based on experience, the works of Ackermann (1980), Ayeni (1982), Li (1992), Gao (1997) and Davis *et al.* (2001) can be referred to. In these empirical models regression techniques are used to adjust the different parameters of the model to the experimental results obtained, generally on vast terrain databases. As an example of a classical methodology in the development of this type of model, we can highlight Gao's work (1997), where the accuracy (root mean square error (RMSE)) of the DEMs extracted from topographic maps was regressed against contour density ($\mathrm{km\,km^{-2}}$) and DEM resolution at six resolution levels. More recent studies like that of Davis *et al.* (2001) use characteristics which are typical of the Digital Photogrammetric Workstations (DPWs) for modelling the accuracy of grid DEMs. It is an interesting empirical model capable of estimating both the global error of the DEM (RMSE) and the vertical accuracy of the elevation value for every grid point in the DEM (spatial variation of elevation error). For this purpose, they use parameters derived from the automated DEM extraction, called figure of merit (FOM), as independent variables in the regression analysis. An FOM value is

produced for each DEM point by the stereo-correlation software used in the DEM generation process. Obviously, this model is highly dependent upon the methods used for computing FOM values and would only be suitable when the stereo-matching method is being utilized to obtain the DEM.

In the case of theoretical models, the first relevant contributions were based on relatively complex mathematical formulations such as the Fourier analysis (Makarovic 1972) and autocovariance and variogram analysis (Kubik and Botman 1976). In the first case, no suitable mathematical expressions were derived for practical application, whilst in the second, it should be stressed that it is difficult to have good approximate co-variance values as a terrain descriptor, and therefore the final prediction would not be very reliable (Li 1993a).

Since the 1990s, it has been possible to observe a certain tendency to develop theoretical models based on the error-propagation theory, segmenting the problem and calculating separately the error contributed by the different uncertainty sources. In the case of Weng's proposal (2002), the total DEM uncertainty is determined from cartographic digitising, as the square root of the sum of the RMSE squares related to three sources of error: topographic map source, sampling and measurement error, and interpolation process. Likewise, Filin and Doytsher's work (1998) can be quoted, where a thorough and mathematically complex theoretical model is developed based on the propagation error of the photogrammetric solution process.

A special mention is made of the studies carried out by Li (1993a, b), as they have provided the basis for the theoretical development of the model presented in this paper. In these studies, theoretical models are based on the distinction between the error ascribable to measuring the sample data points, which from now on will be referred to as σ^2_{SDE} or sample data error, and the sum of the interpolation error and the error due purely to sampling the continuous terrain surface with a finite grid interval (σ^2_{IL}). The latter is sometimes referred to as information loss (Huang 2000). It is important to note that both terms are expressed as error variance.

Of the two terms mentioned, σ^2_{SDE} is relatively easy to obtain from empirical observations. For example, in photogrammetric DEM generation, the photographic scale is the main determinant of DEM accuracy given that all other specifications are logically consistent. In this case, σ^2_{SDE} can be estimated with reasonable approximation from the Flying Height above Mean Terrain (H). Torlegard *et al.* (1986) evaluating the sampling error as 0.2–0.4‰ (per mill) of the flight height H for flat terrain and 1–2‰ H for mountainous terrain. In the case of DEM generation using DPWs, a high precision of $\sigma_{SDE}<0.1$‰ H can be achieved for manual measurement (Karras *et al.* 1998). For elevations collected automatically with a cursor kept on the terrain by digital correlation, the precision obtained could be $\sigma_{SDE}<0.2$‰ H (Karras *et al.* 1998). The typical specification for vertical error is a σ_{SDE} of $H/9000$ and a maximum error of three times σ_{SDE} (Daniel and Tennant 2001).

Likewise, theoretical approximations based on space resection projective geometry can be used, obtaining equations like the following (Saleh and Scarpace 2000):

$$\sigma_{SDE} = G_r \sigma_p \frac{H}{f} \frac{H}{B} \tag{1}$$

G_r being the geometric resolution of the digital image (mm pixel^{-1}), f the camera

focal length (mm), σ_p the parallax precision (pixels) and H/B the base-to-distance ratio of the photogrammetric flight. Values of σ_p between 0.4 and 0.7 pixels are frequent in DPW automatic DEM generation (Karras *et al.* 1998).

Nonetheless, the estimation of σ_{IL} presents greater problems because terrain shape varies from place to place, i.e. 'terrain is highly capricious'. Therefore, it is impossible to find an analytical method to compute the standard deviation for all the height differences (δh) between the terrain surface and the DEM surface (σ_{IL}). Li (1993b) proposes the use of statistical methods where the random variable is δh. However, the model proposed by Li (1993b) requires the estimation of a series of parameters which depend to a great extent on the morphology of the terrain, a circumstance which is not resolved in the above-mentioned study.

One alternative to theoretical or empirical models for modelling information loss could be that pointed out in Huang's (2000) paper. This study proposes the utilization of the possibilities offered by powerful DPWs to generate an extremely dense set of points derived directly from stereo-correlation. This DEM can be as dense as one point every few pixels. Therefore, the DEM can be treated as a representation of the terrain free from information loss, i.e. it could be considered as a very good reference surface for assessing the information loss in a less dense DEM. This is a practical, simple, and interesting methodology that can only be applied if we have a DPW. Moreover, to estimate the accuracy of a grid DEM with a certain spacing, it would be necessary to obtain previously an extremely dense DEM of the same terrain.

In this paper, the estimation of σ_{IL} was approached by an empirical approximation, where the most important factors that intervene in the vertical accuracy of a grid DEM are taken into account, such as sampling interval and terrain complexity (Li 1992, Gong *et al.* 2000, Aguilar *et al.* 2005). Previously, the modelling method was fixed as triangulation with linear interpolation, and the error variance of the data source (σ^2_{SDE}) was included in the theoretical model.

2. Methodology

2.1 *Study sites and data sets*

The two study areas are located in Almería, south-eastern Spain. The first is situated in what is known as the 'Comarca del Mármol', specifically in the municipal area of Macael. It is a zone with marble quarries and a high level of extraction activity which has formed a terraced and artificial relief; hence the predominance of steep slopes and even vertical walls that are found there. The second study area is situated in the 'Comarca del Campo de Níjar', bordering on the 'Cabo de Gata' Nature Reserve. This is an area with a smooth relief sculpted by natural agents. For the development of this study, eight topographic surfaces were selected, measuring 198×198 m (approximately 3.92 ha), two situated in Macael, and six in Níjar. The morphological characteristics of these surfaces can be observed in table 1. It is interesting to observe the great diversity of the morphologies utilized, in terms of their roughness and their average slope. As a roughness descriptor, we used the Standard Deviation of Unitary Vectors perpendicular to the topographic surface (SDUV), calculated as detailed in section 2.4.

The DEM of each topographic surface was obtained automatically by stereo-image matching. Later on, a revision and a manual edition of the DEM were carried out. The photogrammetric flight presented an approximate scale of 1 : 5000 and was

Table 1. Characteristics of the topographic surfaces studied[a].

Terrain descriptive statistics	Níjar						Macael	
	Smooth hillside	Flat	Rolling1	Rolling2	Slightly mountai-nous	Mountai-nous	Steep-rugged hillside	Highly rugged
DEM size (2×2 m spacing)	10 000	10 000	10 000	10 000	10 000	10 000	10 000	10 000
Average elevation (m)	120.25	166.54	176.94	195.42	178.96	215.16	762.29	922.5
$Z_{max}-Z_{min}$ (m)	9.06	6.70	17.25	23.08	34.43	45.17	201.32	116.48
Elevation coefficient of variation (%)	2.01	0.97	2.28	2.20	3.79	3.98	6.52	4.28
Average slope (%)	4.52	3.30	9.27	10.01	19.42	31.18	82.14	65.12
Slope coefficient of variation (%)	17.76	48.02	45.66	69.59	58.62	38.27	30.91	77.01
SDUV (m)	0.02	0.03	0.09	0.10	0.19	0.31	0.35	0.64

[a]The standard deviation of unitary vectors perpendicular to topographic surface is denoted by SDUV.

carried out with a Zeiss RMK TOP 15 metric camera using a wide-angle lens with a focal length of 153.33 mm. The negatives were digitalized with a Vexcel 5000 photogrammetric scanner with a geometric resolution of 20 μm and a radiometric resolution of 24 bits (8 bits per RGB channel). In the case of the Níjar study area, the DEM was constructed using the module *Automatic Terrain Extraction* of the digital photogrammetric system LH Systems SOCET SET NT 4.3.1®. For the study area of Macael, the DEM was constructed using the modules *ImageStation Automatic Elevations* and *ImageStation DTM Collection* of the digital photogrammetric system Z/I Imaging ImageStation SSK®. In both cases, we obtained a final DEM in grid format with a spacing of 2×2 m, orthometric elevations, map projection UTM zone 30 North and *European Datum* 1950.

2.2 *Theoretical approach*

The theoretical development presented is similar to that proposed by Li (1993b) and used by other authors like Huang (2000). In Li's paper (1993b), the error made when modelling the terrain surface is determined using contiguous bilinear facets supported by square grid sample data. In our case, randomly spaced data points are converted into regularly gridded data points using triangulation with linear interpolation, i.e. we use contiguous triangular facets to obtain regular grid DEMs. In figure 1, a facet can be observed from the triangular grid established with the use of the optimal Delaunay triangulation (Guibas and Stolfi 1985). This algorithm creates triangles by drawing lines between data points. The original points are connected in such a way that no triangle edges are intersected by other triangles. The result is a patchwork of triangular facets over the extension of the grid.

The overall average value of error variances for all the points along the whole AB (σ^2_{AB}) profile, where A and B are sample data, can be modelled by the equation

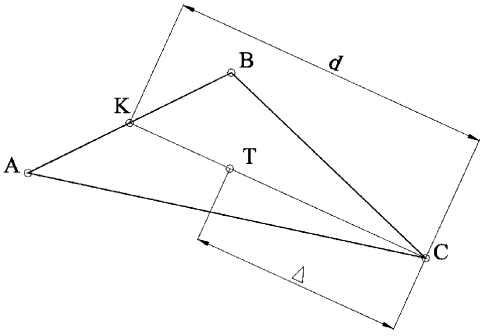

Figure 1. Linear interpolation of point T belonging to the triangular facet of sample points A, B, and C.

proposed by Li (1993b):

$$\sigma^2_{AB} = \frac{2}{3}\sigma^2_{SDE} \tag{2}$$

Where σ^2_{SDE} is the sample data error, expressed as error variance. The introduction of the sample data error into the theoretical model is crucial, since the results obtained by Filin and Doytsher (1998) have shown that ignoring the accuracy estimate of the measurements can lead to biased results. However, for the overall accuracy of any point K belonging to the AB profile, another term should be added:

$$\sigma^2_{K} = \frac{2}{3}\sigma^2_{SDE} + \sigma^2_{IL} \tag{3}$$

σ^2_{IL} being the information loss, i.e. the error due purely to sampling with a finite grid interval and using linear interpolation for modelling terrain surface (Huang 2000). The derivation of equation (3) is based on the general error-propagation theory (expressed as error variance), assuming that the sources of error (sample data error and information loss) are independent or uncorrelated and, besides, that the errors are randomly distributed (Li 1993b, Huang 2000, Weng 2002).

The calculation of the overall accuracy of height Z at point T (Z_T) can come close to determining the error made when linearly interpolating profile KC, C being the third sample point of the triangle. From figure 1, the following expression can be deduced:

$$Z_T = \left(\frac{d-\Delta}{d}\right) Z_C + \frac{\Delta}{d} Z_K \tag{4}$$

The variance of Z_T, σ^2_T, can be estimated using the general error propagation theory, knowing that C is a sample point, and K is not. Therefore:

$$\sigma^2_T = \left(\frac{d-\Delta}{d}\right)^2 \sigma^2_{SDE} + \left(\frac{\Delta}{d}\right)^2 \sigma^2_K \tag{5}$$

Substituting σ^2_K with its value (equation (3)) and calculating the average value for the variances of all the points in the KC length profile (σ^2_{KC}), we find that:

$$\sigma^2_{KC}(1/d) = \int_0^d \left[\left(\frac{d-\Delta}{d}\right)^2 \sigma^2_{SDE} + \left(\frac{\Delta}{d}\right)^2 \left(\frac{2}{3}\sigma^2_{SDE} + \sigma^2_{IL}\right)\right] d\Delta \tag{6}$$

Solving the integral proposal, we obtain:

$$\sigma^2_{KC} = \frac{5}{9}\sigma^2_{SDE} + \frac{1}{3}\sigma^2_{IL} \tag{7}$$

Notice that the term σ^2_{IL} must be added again to obtain the overall accuracy of the points along profile KC, an expression that allows us to determine the average value for the error of the points on a triangulated surface given as error variance, σ^2_{surf}.

$$\sigma^2_{surf} = \frac{5}{9}\sigma^2_{SDE} + \frac{4}{3}\sigma^2_{IL} \tag{8}$$

The sample data error, σ^2_{SDE}, evidently depends on the method employed to obtain sample points.

2.3 *Evaluation of the grid DEM accuracy*

As we discussed in the previous section, we only need to estimate the value of σ_{IL} to evaluate the grid DEM error, σ_{surf}, because σ_{SDE} can be obtained from empirical observations depending on the method used to measure the sample data points. If the sample data points are considered free of error, the following expression is deduced:

$$\sigma^2_{surf} = \frac{4}{3}\sigma^2_{IL} \tag{9}$$

Because the most widely used global accuracy measure for evaluating the performance of DEMs is the RMSE (Li 1988, Wood 1996, Yang and Hodler 2000), and bearing in mind that the RMSE is close to the value of σ_{surf} when the mean of residuals tends to be zero (unbiased residuals), we can write the following equation:

$$RMSE_{surf} = \frac{2}{\sqrt{3}}RMSE_{IL} \Rightarrow RMSE_{IL} = \frac{\sqrt{3}}{2}RMSE_{surf} \tag{10}$$

That is to say, estimating $RMSE_{surf}$ when the sample data points are considered free of error ($\sigma_{SDE}=0$), we obtain an indirect measure of the value of the information loss ($RMSE_{IL} \approx \sigma_{IL}$).

In figure 2, we can observe the flow chart of the procedure employed for computing $RMSE_{surf}$ using the true validation method (Voltz and Webster 1990), always considering the check points as free of error. We notice that the residuals at the M check points (randomly sampled) can be spatially autocorrelated. This property of the DEM error has been reported by several authors (Wood 1996, Fisher 1998, Weng 2002). In fact, if the residuals at the check points are not independent, we could state that the true sample size is lower than that of the *M* check points. Therefore, the use of a data set of *M* spatially autocorrelated residuals would lead to an $RMSE_{surf}$ variability which is lower than it should be. Thus, we checked the degree of spatial autocorrelation for every residual data set with a semivariogram (Aguilar *et al.* 2005). As a general rule, we found a typical transitional semivariogram with range, nugget, and sill that were fitted to a spherical model. The lower range computed was around 20 m. Therefore, if the distance separating two check points is greater than the range, then the residuals measured at those check points are not spatially autocorrelated. For this reason, a pseudo-random algorithm was designed for the extraction of check points, imposing the condition that the separation between the points extracted should be at least 20 m. A final value of 73 check points was obtained for each control data set, corresponding to the minimum value computed for the eight data sets.

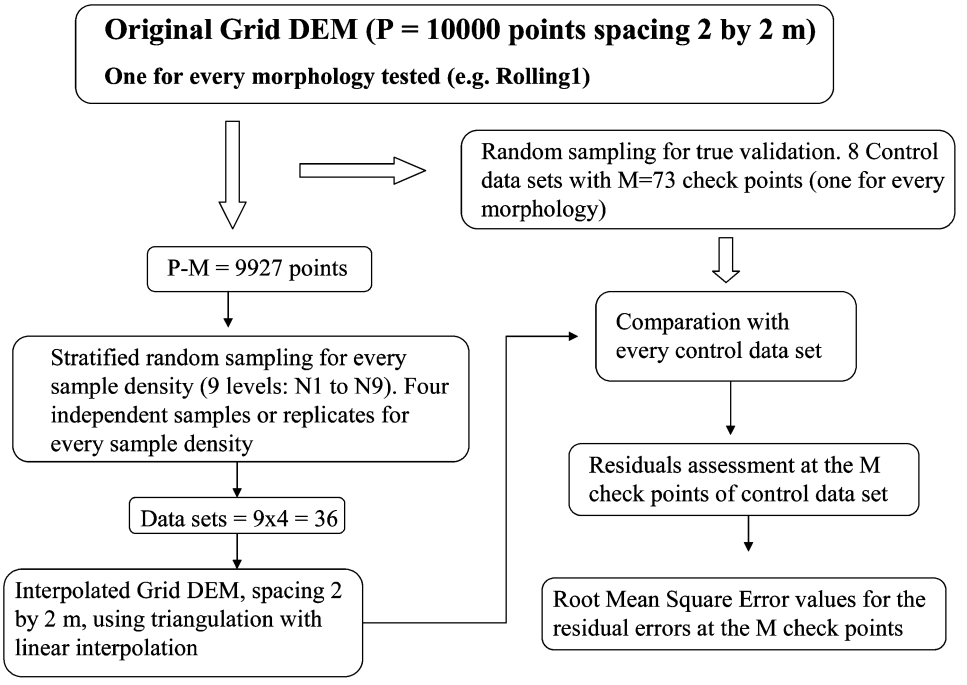

Figure 2. Flow chart of the scheme used to evaluate $RMSE_{surf}$.

The different sampling densities tested were obtained from the original DEM of each morphology by stratified random sampling (4×4 sampling quadrants). In table 2, we can see the nine sample densities contemplated (N1 to N9) and their equivalent spacing in a regular grid. For each sample density, four repetitions were extracted, showing a total of $4 \times 9 = 36$ initial data sets for each morphology tested (figure 2).

Once the initial data sets were obtained, a 2×2 m spacing grid DEM was generated for each data set using triangulation with the linear interpolation method. The residuals of each DEM were assessed over the 73 check points previously selected in each morphology, obtaining the vertical RMSE ($RMSE_{surf}$ estimated) as observed variable, calculated according to equation (11):

$$RMSE_{surf} = \sqrt{\frac{\sum_{i=1}^{73} \left(Z_{icp} - Z_{iDEM}\right)^2}{73}} \tag{11}$$

Table 2. Sample densities, N1 to N9, composed of scattered sample data from stratified random sampling[a].

Sample size	Sample density								
	N1	N2	N3	N4	N5	N6	N7	N8	N9
Points	36	84	196	292	964	1444	1924	2884	4804
Points m^{-2}	0.00091	0.00214	0.005	0.00744	0.02459	0.03683	0.04908	0.07357	0.12255
ES (m)	33.1 × 33.1	21.6 × 21.6	14.1 × 14.1	11.6 × 11.6	6.3 × 6.3	5.2 × 5.2	4.5 × 4.5	3.7 × 3.7	2.8 × 2.8

[a]ES: equivalent spacing in grid format.

where Z_{icp} is the check point elevation, and Z_{iDEM} is the interpolated grid DEM elevation.

2.4 *Definition and processing of terrain roughness descriptors*

As variables that are representative of the topographic surface morphology, the following descriptors were selected: average terrain slope (AS), standard deviation of terrain slope (SDS), standard deviation of unitary vectors perpendicular to the topographic surface (SDUV), standard deviation of the height difference between adjacent samples in the DEM (SDHD), and finally the roughness estimation by first, second, and third degree surface fitting error (SFE1, SFE2, and SFE3). The processing and detailed calculation of each one of these are described below.

First, we proceeded to fill in the grid using triangulation with linear interpolation from the original sample points (N1 to N9 sampling densities). The appropriate triangulated irregular network was obtained by the optimal algorithm Delaunay triangulation (Guibas and Stolfi 1985). A final grid DEM with a spacing of 2×2 m was obtained for each original data set, to be considered as input for computing the descriptors AS, SDS, SDUV, and SDHD. The calculation of descriptors SFE1, SFE2, and SFE3 was carried out over the original sample data, i.e. without interpolation.

2.4.1 Average Terrain Slope (AS). Starting from the 2×2 m spacing grid DEM, the slope (S_{ij}) was determined in each node of the grid using the gradient calculation:

$$S_{ij} = \sqrt{\left(\frac{\partial z}{\partial x}\right)^2 + \left(\frac{\partial z}{\partial y}\right)^2} \tag{12}$$

The third-order finite difference method shown in equation (12) is more accurate than some of the others (Skidmore 1989) and was therefore chosen for this study. Using the compass-based grid notation difference, equation (12) yields:

$$S_{ij} \approx \sqrt{\left(\frac{Z_E - Z_W}{2\Delta x}\right)^2 + \left(\frac{Z_N - Z_S}{2\Delta y}\right)^2} \tag{13}$$

where Z_E, Z_W, Z_N, and Z_S are the elevations of the four cardinal points (east, west, north and south) neighbours in each node in the grid DEM. Δx and Δy represent the spacing of the grid DEM, 2 m in our case.

The value of the average terrain slope descriptor would be the arithmetical mean of the slopes calculated in every node in the grid, excluding the edge values (first and last rows, first and last columns).

2.4.2 Standard deviation of terrain slope (SDS). The standard terrain slope deviation was computed in radians from the slope values on each node of the grid DEM obtained in the previous section:

$$SDS = \sqrt{\frac{\sum_{\forall i, \forall j} (S_{ij} - AS)^2}{N}} \tag{14}$$

with N being the number of points in the grid DEM, S_{ij} the terrain slope at the point located in row i and column j, and AS the average terrain slope.

2.4.3 Standard deviation of unitary vectors perpendicular to the topographic surface (SDUV). Once the slope had been determined at each point in the grid DEM, its aspect was calculated. The algorithm for computing terrain aspect calculates the downhill direction of the steepest slope at each grid node. The aspect at each grid node was calculated as angle θ_{ij}, expressed in degrees, which exists between direction north and the projection on the horizontal plane of the slope vector normal to the surface. That is to say, 0° points to the north and 90° points to the east:

$$\theta_{ij} \approx 270 - \tan^{-1}\left(\frac{\frac{Z_N - Z_S}{2\Delta y}}{\frac{Z_E - Z_W}{2\Delta x}}\right) \tag{15}$$

The SDUV was computed determining the variance of the unitary vectors which are perpendicular to the surface in each node (*i*,*j*) in the grid DEM (adapted from Hobson 1972). The Cartesian components $x_{i,j}$, $y_{i,j}$, and $z_{i,j}$ of each unitary vector can be expressed in terms of slope S_{ij} and aspect θ_{ij} in this node through the following expressions:

$$\begin{aligned} x_{ij} &= \sin(\gamma_{ij})\sin(\theta_{ij}) \\ y_{ij} &= \sin(\gamma_{ij})\cos(\theta_{ij}) \\ z_{ij} &= \cos(\gamma_{ij}) \\ \gamma_{ij} &= \tan^{-1}(s_{ij}) \end{aligned} \tag{16}$$

This way, we were able to find the variance of the unitary vectors for each co-ordinate *x*, *y*, *z*, and determine the total standard deviation (SDUV) using the following expression:

$$\text{SDUV} = \sqrt{\text{variance}(x) + \text{variance}(y) + \text{variance}(z)} \tag{17}$$

2.4.4 Standard deviation of the height difference between adjacent grid points in the DEM (SDHD). The standard deviation of the height difference between adjacent grid points in the DEM has been used as terrain roughness descriptor by some authors (Evans 1972, Rees 2000). The algorithm used in our case starts from the interpolated grid DEM with a 2×2 m spacing. A 3×3 node mobile window was shifted over the whole of the interpolated grid DEM. Then, the average height difference between the central node of the window and the rest of the nodes (eight closest neighbours) was calculated according to the following expression:

$$\Delta Z_P = \frac{\sum_{k=1}^{8} |Z_P - Z_k|}{8} \tag{18}$$

Where Z_P is the elevation at the central point of the window (node *P*) and Z_k is the elevation of each of the eight points surrounding node *P*. Thus, a mean value of the height differences around each node of the grid DEM was obtained. The SDHD is defined as the standard deviation of the set of values ΔZ_P.

2.4.5 Roughness estimation by first-, second-, and third-degree surface-fitting error (SFE1, SFE2, and SFE3, respectively). The fitting of a first-, second- or third-degree surface to the irregular sample point grid of the original DEM can be an indicator of

the terrain roughness (Hobson 1972). In fact, if the regression coefficient R^2 is determined for each fitting, a non-dimensional indicator of the terrain roughness could be generated using the simple expression $SFE=1-R^2$. This indicator will be included between values 0 (optimal fitting of the surface⇒less roughness) and 1 (worst fitting⇒maximum roughness).

All the procedures described above were programmed with the SCRIPTER® module, included in the SURFER 8.01® (Golden Software Inc. 2002), which allows the use of the tool Active X Automation to work with the SURFER modelling engine in an environment that is compatible with Visual Basic®.

3. Relationships between DEM accuracy, sampling density, and terrain roughness

First, and foremost, we shall examine the relationships between DEM error, sampling density, and terrain roughness to explore the morphology that our empirical model should have. For this purpose, six morphologies were selected from the eight that were available, in order to establish and calibrate the different empirical models tested to estimate the $RMSE_{surf}$ considering the sample points as free of error. The morphologies chosen were the following: smooth hillside, rolling1, slightly mountainous, mountainous, highly rugged, and steep-rugged hillside (table 1). The two remaining morphologies, flat and rolling2, would be used to carry out the validation of the empirical models developed.

3.1 *DEM error and sampling density*

In figure 3, we can observe the relationship between RMSE and sample density N for the slightly mountainous and steep-rugged hillside morphologies. The variation of RMSE with increase in sample density is reasonably fitted to a potential decreasing function, a circumstance observed in other studies (Wang 1990, Aguilar *et al.* 2003), which will be fundamental in the structure of the final model.

Table 3 shows the fitting parameters of the potential decreasing model for the data observed for each of the six morphologies tested. We can appreciate high regression coefficients which reflect the goodness of the fitting in morphologies as different as smooth hillside and steep-rugged hillside.

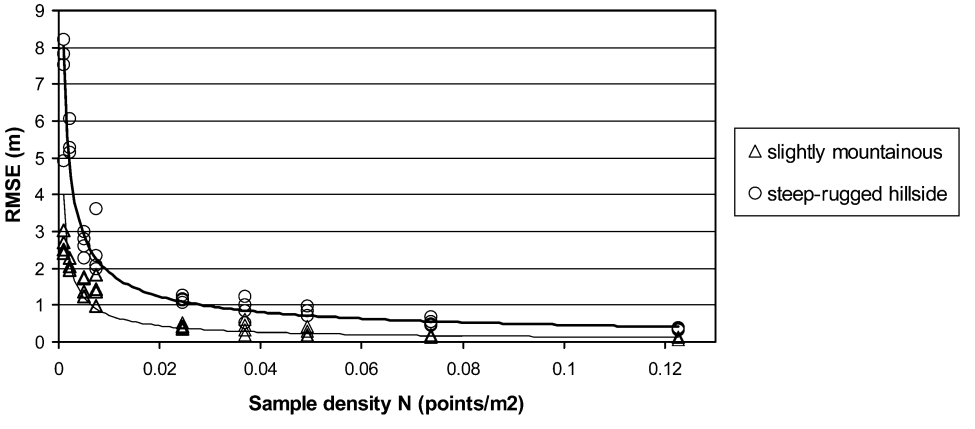

Figure 3. Relationship between $RMSE_{surf}$ and sample density N for the morphologies Slightly mountainous and Steep-rugged hillside.

Table 3. Parameters of the decreasing potential model adjusted to the relationship between $RMSE_{surf}$ (m) and sampling density N (points m^{-2}): $RMSE_{surf}=a.N^{-b}$.

Morphology	Parameter a	Parameter b	Regression coefficient R^2
Smooth hillside	0.0035	0.5929	0.92
Rolling1	0.0072	0.7420	0.95
Slightly mountainous	0.0269	0.7158	0.91
Mountainous	0.0379	0.6954	0.95
Highly rugged	0.8039	0.4480	0.88
Steep-rugged hillside	0.1155	0.6063	0.95

In sections 3.2 and 3.3, the most suitable terrain roughness descriptors to explain the relief effect on the DEM error will be selected to be included in the model.

3.2 *Terrain roughness and sampling density*

In the first place, it seems reasonable to request a certain independence from the terrain descriptor with regard to the spatial distribution and number of original sample points in the dataset. Thus, the final user of the model can determine the approximate value of the appropriate descriptor using data previously extracted from topographic maps (Gao 1995) or DEMs (e.g. in USA: National Elevation Dataset at the USGS Earth Resources Observation Systems Data Centre; Gesch *et al*. 2002). In table 4, one can verify how the descriptors presenting a lower variability with regard to the number and distribution of sample points are Average Slope and SDUV. The value calculated for descriptor SDHD is shown as relatively sensitive to the number and distribution of sample points, especially in the case of mountainous and slightly mountainous morphologies with coefficients of variation higher than 28%.

In any case, the coefficients of variation calculated show promising results, especially bearing in mind the range of sample densities employed (from N1=0.00091 points m^{-2} to N9=0.12255 points m^{-2}). In figure 4, we can observe how the variability in determining descriptors SDUV and SDHD is high, above all

Table 4. Coefficient of variation (%) of the different roughness descriptors tested for every terrain dataset[a].

	Coefficient of variation (%) of roughness descriptor						
Terrain	SDUV	SDHD	SDS	Average Slope	SFE1	SFE2	SFE3
Smooth hillside	10.39	17.17	15.13	1.67	8.79	12.38	17.41
Rolling1	8.20	13.71	10.10	5.14	8.51	7.27	8.90
Slightly mountainous	6.12	28.54	10.14	4.91	8.28	8.27	14.86
Mountainous	4.35	39.19	16.21	5.28	2.60	11.39	9.43
Highly rugged	1.92	12.01	5.10	6.45	5.40	3.61	12.18
Steep-rugged hillside	8.71	18.33	11.92	2.22	21.50	21.22	8.39
Mean value	6.61	21.49	11.43	4.28	9.18	10.69	11.86

[a]The coefficient of variation for every descriptor has been computed using 36 values (4 replicates × 9 sample densities).

in the case of SDHD for low sample densities (N1 to N4). Starting from sample density N5, with an equivalent spacing of 6.3 m in grid format, the values of both descriptors are quite independent from the sample size and the spatial distribution of sample points because the reliability intervals are very narrow.

3.3 *DEM error and terrain roughness*

Second, a good descriptor of the terrain morphology incidence on the DEM error should present a high relationship with the RMSE of this DEM. A relationship can be observed between the RMSE and the different terrain descriptors which is very close to an increasing potential function (figure 5), with high regression coefficients. However, it must be noted that the independent observations are not well distributed in many instances because of the deficient distribution of the descriptor values. In fact, in figure 5, we can see that large clumps of low SDHD values are offset by a few high values. Average Slope and SDS have similar problems. This poor distribution of independent observations can inflate the regression coefficients unrealistically. Thus, it would be desirable to have at our disposal a vast set of morphologies uniformly representing the whole roughness spectrum (see section 7).

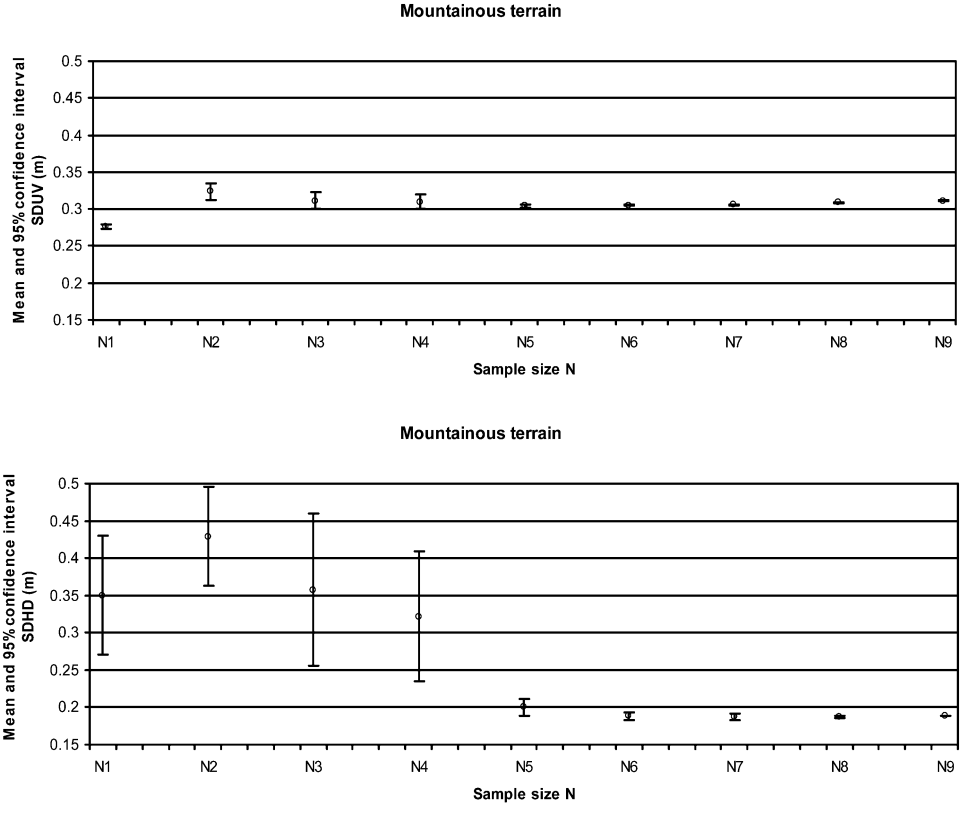

Figure 4. Relationship between SDUV and sample size (top) and SDHD and sample size (bottom) for mountainous terrain. Both roughness descriptors are showed as the mean value and 95% confidence interval.

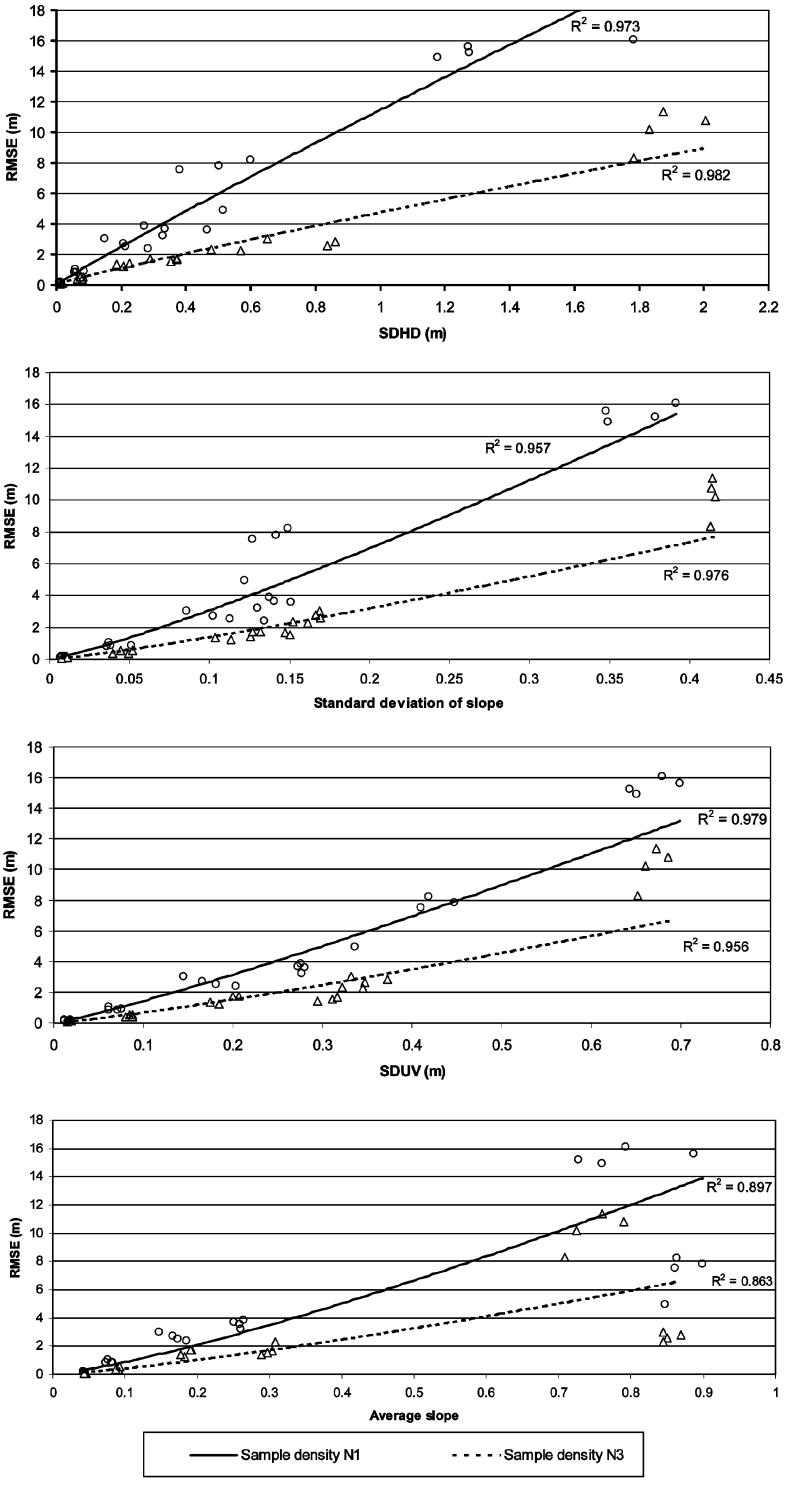

Figure 5. $RMSE_{surf}$ with respect to several roughness descriptors at sample densities N1 (○) and N3 (△). The relationship between RMSE and roughness descriptors is adjusted to an increasing potential function $RMSE_{surf}=a.D^b$, where D is the descriptor.

In any case, using only the Average Slope terrain descriptor R^2, values lower than 0.90 were obtained, due to a defective fitting of the model to the morphologies in the Macael site. Let us recall that these morphologies are constituted by quarry terrains with a terraced and anthropic relief, where steep slopes and even vertical walls are predominant (table 1).

On the other hand, the group of descriptors SFE1, SFE2, and SFE3 showed very low regression coefficients, lower than 0.50 in each case. The inefficiency shown by the terrain descriptor Surface Fitting Error for the modelling of the DEM error is due to the fact that it presents a high dependence on the morphological analysis scale. When we seek to fit a first-, second-, or third-degree surface to terrain with homogenous behaviour on a large scale, a hillside for example (steep-rugged hillside), excessively low SFE values are obtained. That is to say, the local roughness is underestimated. Conversely, let us suppose we wish to fit a first-degree surface, a flat surface, to the triangular transversal section of a riverbed. In this case, the fitting will be deficient, and therefore SFE1 will adopt a very high value, although the local roughness of the riverbed is actually very low.

4. Development of empirical models

Once the relationships between the variables involved in grid DEM error modelling have been described, we can conclude that the structure of the empirical model should conform starting from the product of two potential functions, increasing in the case of the terrain descriptor and decreasing in the case of the sampling density. In table 5, we can observe the models proposed together with the calibration parameters obtained by nonlinear regression. The Marquardt iterative search algorithm was used to determine the estimates that minimize the residual sum of squares (Draper and Smith 1981).

Table 5. Description of developed empirical models for every roughness descriptor tested[a].

Descriptor	MAE (m)	SDR (m)	Empirical model	Parameters			Regression coefficient
				a	*b*	*c*	R^2
SDUV	0.43	0.63	$RMSE_{surf} = a.SDUV^b.N^{-c}$	2.3175	1.71739	0.38001	0.9618*
Average Slope	1.08	1.79	$RMSE_{surf} = a.AS^b.N^{-c}$	0.73825	0.89145	0.41707	0.6929*
SDHD	0.38	0.7	$RMSE_{surf} = a.SDHD^b.N^{-c}$	0.41684	0.95062	0.47034	0.9533*
SDS	0.45	0.76	$RMSE_{surf} = a.SDS^b.N^{-c}$	2.69652	1.31622	0.44464	0.9442*
SFE1	1.83	2.62	$RMSE_{surf} = a.SFE1^b.N^{-c}$	0.45966	0.28757	0.42769	0.3421*
SFE2	1.73	2.47	$RMSE_{surf} = a.SFE2^b.N^{-c}$	0.91912	0.56598	0.40632	0.4151*
SFE3	1.76	2.51	$RMSE_{surf} = a.SFE3^b.N^{-c}$	0.86444	0.43959	0.43158	0.3996*

[a]$RMSE_{surf}$ is expressed in metres and sample density (N) in points m^{-2}. SDUV and SDHD are expressed in m and SDS in radians. Average Slope, SFE1, SFE2, and SFE3 are non-dimensional. MAE: Mean Absolute Error. SDR: Standard Deviation of Residuals. *Significant at the 0.01 level.

One can verify how parameter 'c' of the potential decreasing function presents similar values in every model developed, indicating that the variation of the RMSE with sampling density N is independent of the type of terrain descriptor employed.

On the other hand, one can see how the models containing descriptors SDUV, SDHD, and SDS present very acceptable results with R^2 regression coefficients higher than 0.94. However, in the case of the SFE group of descriptors, low R^2 values have been obtained, thus confirming their inefficacy to model DEM error for the reasons stated in section 3.3.

Equally, the model that employs Average Slope as descriptor offered a mediocre fitting to the data observed, as also pointed out in section 3.3 (figure 5). No doubt, the inclusion of extremely rugged terrain such as that situated in the marble quarries of Macael, with very steep slopes and terraced and anthropic morphology, has decreased the efficacy of Average Slope to model the RMSE of the grid DEM generated.

Based on experimental tests, Ackermann (1980) established that the relationship between DEM error and sampling interval is linear. Likewise, he obtained linear relationships between the mean slope of an area and the error of a DEM. Both findings led him to formulate the following model.

$$\sigma^2_{\mathrm{DEM}} = K_1\sigma^2_{\mathrm{raw}} + K_2(\mathrm{D}_x\tan\alpha)^2 \tag{19}$$

where D_x denotes the sampling interval, $\tan\alpha$ is the mean slope of the area, $\sigma^2{}_{\mathrm{raw}}$ is the error variance of raw data (error of sample data measurements), and $\sigma^2{}_{\mathrm{DEM}}$ is the error variance of the final DEM. Parameters K_1 and K_2 were later added by Li (1993a). If the sample data points are supposed to be free of error ($\sigma^2{}_{\mathrm{raw}}=0$), we have a very similar model to the empirical one proposed in this study where Average Slope is used as descriptor. In fact, applying the equation (19) model to our data, an R^2 value of 0.68 is obtained, a similar value to that presented in table 5. When the data from the two Macael morphologies (steep-rugged hillside and highly rugged) are removed in the regression analysis, the value of R^2 increases to 0.92. Thus, it can be concluded that the Average Slope can be a good roughness descriptor for terrain with geomorphology modelled by natural processes and where slopes are neither extreme nor too variable, at least on a local scale.

The Mean Absolute Error (MAE) and Standard Deviation of Residuals (SDR) values shown in table 5 confirm what has been stated above. Those models based on descriptors SDUV, SDHD, and Standard Deviation of Slope show a lower MAE and SDR than those based on the Average Slope and SFE. That is to say, all the differences between the RMSE values observed and fitted by the model are lower and present moreover a lower dispersion with regard to the mean value. The quantitative differences in the data fitting observed in models SDUV, SDHD, and Standard Deviation of Slope are unimportant, judging by the R^2, MAE, and SDR values. In any case, it must be stressed that although the SDHD model shows a slightly higher dispersion of residuals than model SDUV, the MAE value is lower, which indicates the existence of a series of point residuals with a high absolute value which artificially increases the value of the SDR, hence the decrease in the regression coefficient (see figure 6).

Figure 6 shows the plots of the differences between the observed and the fitted RMSEs for terrain descriptors SDHD, SDUV, Average Slope, and Standard Deviation of Slope. We can highlight how the majority of the empirical models show problems for modelling the RMSEs computed in the steep-rugged hillside and

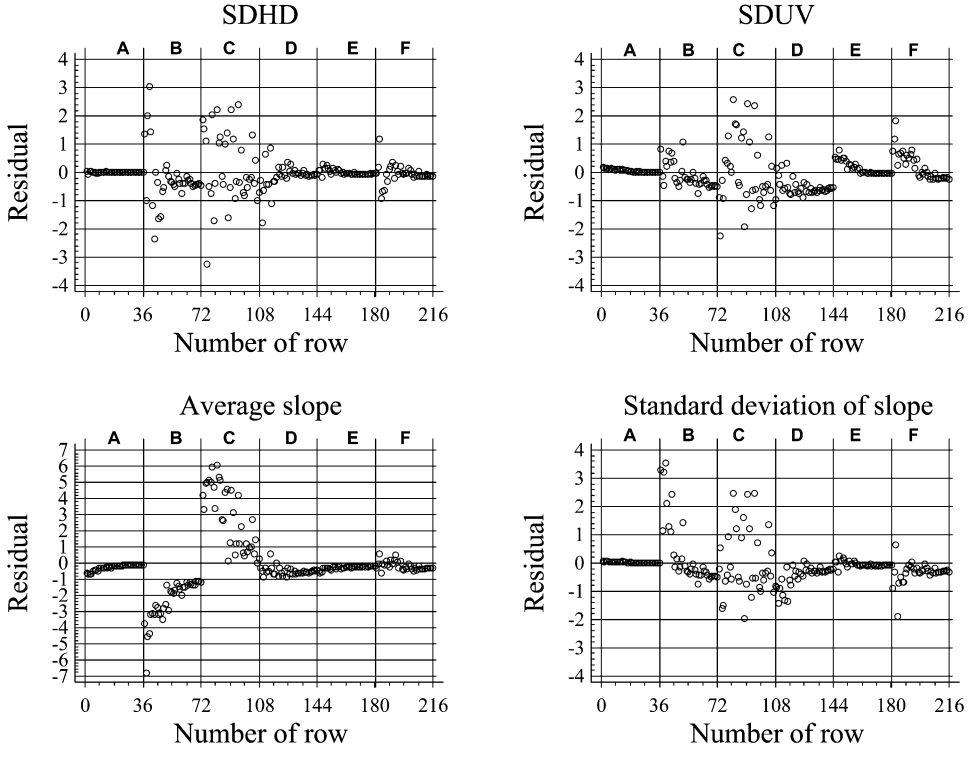

Figure 6. Plots of the differences (m) between the observed and the fitted RMSE values for the empirical models based on the descriptors SDHD, SDUV, AS, and SDS. The horizontal axis shows the rows corresponding to all 216 data sets sorted by morphology (36 data sets) and within every morphology sorted by ascending sample density. A: Smooth hillside; B: Steep-rugged hillside; C: Highly rugged; D: Mountainous; E: Rolling1; F: Slightly mountainous.

highly rugged morphologies of Macael. The errors registered when using the Average Slope model are systematic (overestimation in the case of steep-rugged hillside and underestimation in the case of highly rugged terrain), highly dependent on sampling density (noticeable decrease in error when sampling density increases) and have a high maximum value (between −7 and 6 m). The model based on the Standard Deviation of Slope presents a better fitting to the data observed in the two Macael morphologies, although a certain asymmetry of the residuals can be observed, which indicates a tendency to underestimate the RMSE in these morphologies. On the other hand, this last model fits the mountainous and slightly mountainous morphologies slightly worse than that based on the Average Slope. Although the results offered by models SDHD and SDUV may seem similar *a priori*, a detailed analysis of figure 6 allows us to establish that the model using the SDHD descriptor presents a higher symmetry around the horizontal axis of 0 residual, which indicates the absence of bias in the modelling of the RMSE observed. Thus, when sample densities are low, the SDUV tends to underestimate the RMSE values observed in the rolling1 and slightly mountainous morphologies whilst, at the same time, overestimating the RMSE of the mountainous morphology.

Table 6. Coefficient of variation (CV) of predicted $RMSE_{surf}$ for every morphology and roughness descriptors, computed as $CV=(CV_{N1}+CV_{N2}+\ldots+CV_{N9})/9$, CV_{Ni} being the coefficient of variation for the sample density N_i (four data or replicates).

	Coefficient of variation (%) of predicted $RMSE_{surf}$			
Terrain	SDUV	SDHD	Average slope	Standard deviation of slope
Smooth hillside	10.62	9.41	0.70	11.50
Rolling1	5.71	7.29	1.39	8.26
Slightly mountainous	7.14	12.83	1.91	8.38
Mountainous	2.46	11.41	1.32	5.25
Highly rugged	1.66	5.71	2.06	1.67
Steep-rugged hillside	5.48	10.45	0.83	3.75
Mean value	5.51	9.52	1.37	6.47

Another aspect to be considered in the empirical models developed is the variability of the predicted RMSE with regard to the configuration of the original sample points. All the models developed have shown a mean variability, expressed as coefficient of variation, lower than 10% (table 6), which can be considered acceptable. We must highlight that the relative variability with regard to the sample density shown by the SDHD descriptor (table 4) has been smoothed by the value of parameters 'a' and 'b' obtained in the empirical model fitting (table 5).

Finally, the use of global terrain variability measures only makes sense in calculating the global error of a grid DEM working over the same area where the terrain descriptor has been calculated, i.e. there is an implicit assumption that descriptor variability is stationary across the study area. Obviously, it would be desirable for DEM accuracy to be a local variability function rather than a single, possibly quite misleading, global average. However, it is difficult and sometimes unapproachable, at least in practice, in the mapping production environment. Note that although Slope has been found to be the most important terrain-surface descriptor and is widely used in surveying and mapping (Balce 1987, Li 1993b), it presents a remarkable dependency on the characterization scale. In fact, since the scale is arbitrarily defined and not necessarily related to the scale of characterization required, the derived results may not always be appropriate (Wood 1996). Indeed, Slope is considered scarcely useful to estimate local roughness or to detect variation at a finer scale than DEM. For instance, let us consider two surfaces: one is a plain tilted at 10°. The other is a moderately varying field with an Average Slope of 10°. The two surfaces present the same Average Slope, but their corresponding grid DEMs will probably present a different global error because the local roughness can be remarkably different.

Thus, terrain descriptors more sensitive to changes in local roughness (e.g. SDHD, SDS or SDUV) can perform better than those more centred to describe the roughness variation on a coarser scale (e.g. Average Slope or SFE).

5. Validation of empirical models

Although the observations discussed in the previous section point to the model based on terrain descriptor SDHD as the most appropriate, the results had to be validated on morphologies not used in the calibration of empirical models. This validation was carried out on the flat and rolling2 morphologies (table 1). In

figure 7, we can see the plots of the maximum and minimum RMSE (by means of the 95% confidence interval) versus the sampling density for predicted and observed data on flat terrain. The empirical models based on terrain descriptors SDHD, Standard Deviation of Slope, SDUV, and Average Slope were tested. As we stated previously, the model that best reproduced the data observed on flat terrain was based on the SDHD descriptor, closely followed by the one based on the Standard Deviation of Slope. The SDUV model underestimated the observed RMSE, whereas the Average Slope did the opposite, probably because it was calibrated with a very high Average Slope.

In figure 8, the validation carried out on the rolling2 morphology is shown. The behaviour of the four models developed is similar to that observed on flat terrain, although in this case the SDHD model showed itself as clearly superior to the others. In every model, we can observe a slight overestimation of the observed RMSE at high-level densities. Once more the Average Slope model presented a tendency to overestimate the observed data, a circumstance that in this case can also be seen in the Standard Deviation of Slope.

6. Conclusions

In this study, a theoretical-empirical model has been developed which determines the error that occurs when modelling the terrain surface from randomly spaced data points that are converted into regularly gridded data points using triangulation with linear interpolation. The model consists of a theoretical part based on the error propagation theory, and of an empirical part which attempts to determine the value of what is known as Information Loss ($RMSE_{IL}$), i.e. the error due purely to sampling with a finite grid interval and to using linear interpolation of the terrain surface (Huang 2000). The empirical models developed present a morphology based on the product of two potential functions, an increasing one related to terrain roughness, and a decreasing one related to sample density. Some of the bi-variant empirical models developed explain with reasonable accuracy ($R^2>0.94$) the global error of a grid DEM in terms of Root Mean Square Error. To be specific, the results obtained in this study allow us to highlight the empirical model based on the SDHD terrain descriptor as the one that best reproduces, both on a calibration level and on a validation level, the observed grid DEM error in the majority of the morphologies studied, considering that the sample data points are free of error. Thus, bearing in mind the theoretical development shown in sections 2.2 and 2.3, the average value for the error of a grid DEM linearly constructed from scattered sample data, $RMSE_{surf}$ (m), can be expressed by means of the following equation:

$$RMSE_{surf} = \sqrt{\frac{5}{9}RMSE_{SDE}^2 + \left(0.4168 SDHD^{0.9506} N^{-0.4703}\right)^2} \tag{20}$$

where $RMSE_{SDE}$ is the sample data error, expressed as root mean square error (m), SDHD is the standard deviation of the height difference between adjacent grid points in the DEM (m), and N is the sampling density (points m^{-2}).

Equally, $RMSE_{IL}$ (m) can be determined using the following expression:

$$RMSE_{IL} = \frac{\sqrt{3}}{2} 0.4168 \; SDHD^{0.9506} N^{-0.4703} \tag{21}$$

The findings obtained in this work could be used as a guide for the selection of

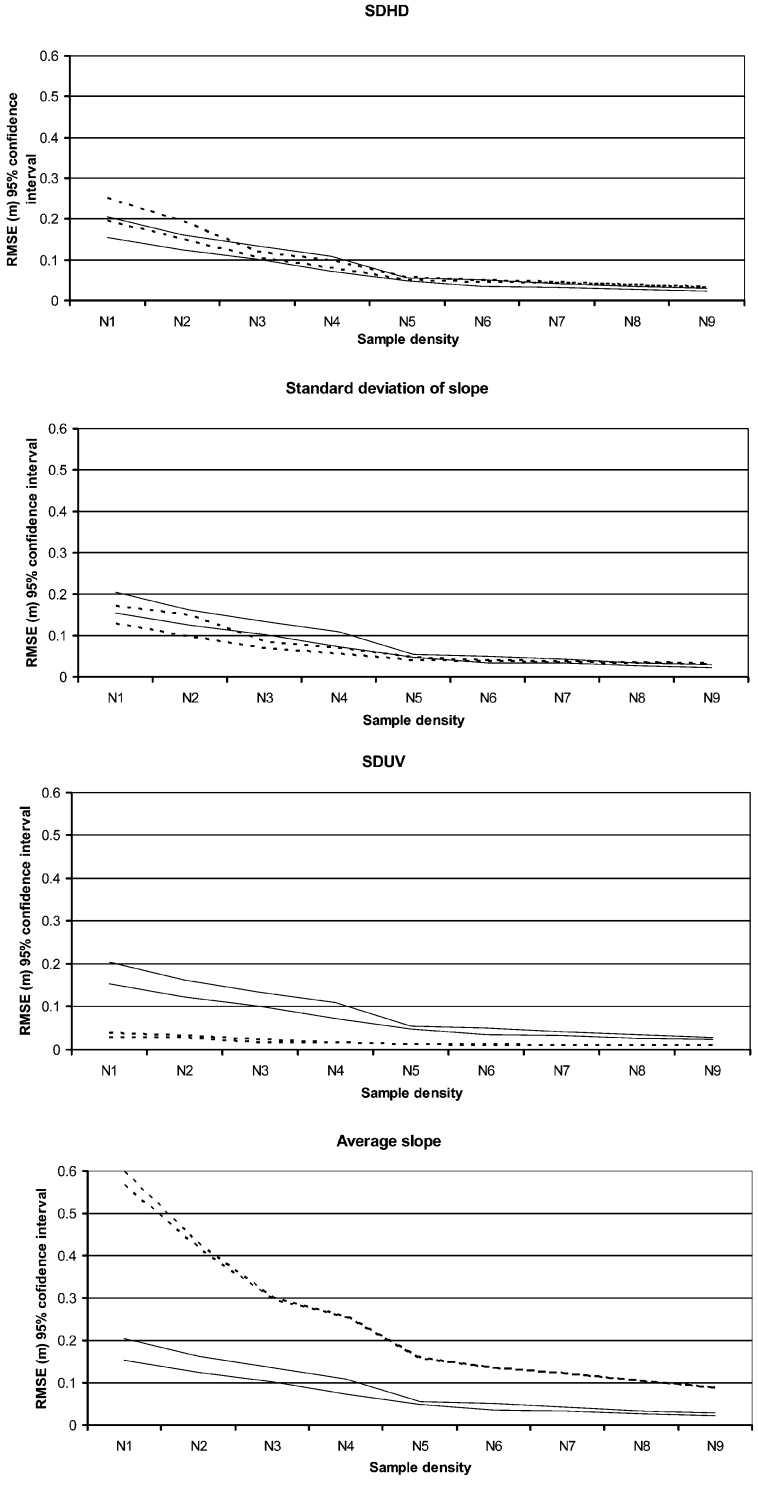

Figure 7. Validation of the models in the case of Flat terrain. Plot of the maximum and minimum $RMSE_{surf}$ (95% confidence interval) versus the sample density and roughness descriptor for predicted data (dashed line) and observed data (continuous line).

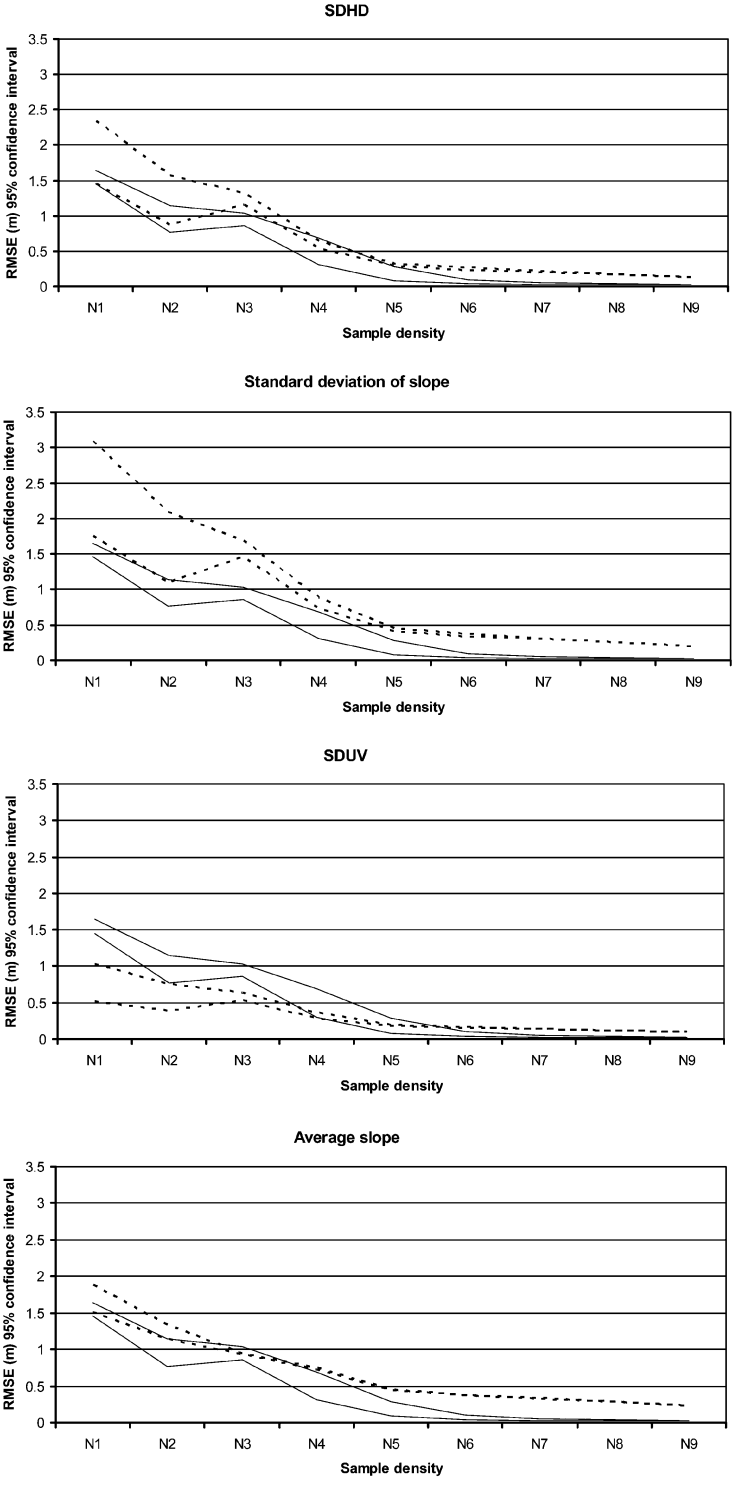

Figure 8. Validation of the models in the case of Rolling2 terrain: plot of the maximum and minimum $RMSE_{surf}$ (95% confidence interval) versus the sample density and roughness descriptor for predicted data (dashed line) and observed data (continuous line).

appropriate resolutions in linearly constructed DEMs from scattered sample data, given the accuracy required and the terrain roughness.

7. Further works

Apart from the descriptors based on the Surface Fitting Error (SFE), which have been proved totally inefficient for modelling the grid DEM error, the rest of the terrain descriptors tested have shown certain advantages and disadvantages. In our case, the SDHD model has proved to be the one that best reproduced the RMSE observed in the eight morphologies studied. We must point out that these morphologies presented a very broad range of slopes and ruggedness, due basically to the inclusion of the quarry soils located in Macael. On the other hand, terrain descriptors Average Slope and SDUV have shown a lower variability than SDHD with regard to the number and distribution of the sample points, which can be considered as favourable elements. In short, it is likely that a single ideal terrain descriptor does not exist for all morphology types that can be found in practice. Each one represents an optimal application range. Thus, we would recommend the inclusion in the empirical model of a particular descriptor with regard to the objective parameters of each terrain, such as its mean slope or its roughness (measured with the SDUV indicator, for example). For the 'à la carte' development of these models we should have at our disposal a vast set of morphologies uniformly representing the whole roughness spectrum. This terrain dataset could be implemented generating synthetic self-similar surfaces with, for example, a fractional Brownian process using a range of values for the fractal dimension (Goodchild and Mark 1987). An infinitely rugged surface should have a limiting fractal dimension of 3, whereas a smooth surface should have a fractal dimension of 2.

Acknowledgements

The authors are grateful to the Consejería de Agricultura y Pesca of the Andalusia Government for financing this work through the Project: 'Cartografía básica para la redacción del proyecto de red de riego del Campo de Níjar (Almería)' (Basic Cartography for the design of the Campo de Níjar irrigation network project). Thanks are also due to Prof. J. Delgado and Prof. J. Cardenal from the University of Jaén (Spain).

References

Ackermann, F., 1980, The accuracy of digital terrain models. In *Proceedings of 37th Photogrammetric Week* (Stuttgart: University of Stuttgart), pp. 113–143.

Aguilar, F.J., Agüera, F., Aguilar, M.A. and Carvajal, F., 2005, Effects of terrain morphology, sampling density and interpolation methods on grid DEM accuracy. *Photogrammetric Engineering and Remote Sensing*, **71**(7), pp. 805–816.

Aguilar, F.J., Agüera, F., Aguilar, M.A., Carvajal, F. and Sánchez, P.L., 2003, Grid digital elevation models accuracy. Analysis and modelling. In *Proceedings of the 13th ADM and 15th INGEGRAF International Conference on Tools and Methods Evolution in Engineering Design* (Naples: Universitá degli studi di Napoli Federico II), CD ROM Proceedings.

Ayeni, O.O., 1982, Optimum sampling for digital terrain models: a trend towards automation. *Photogrammetric Engineering and Remote Sensing*, **48**(11), pp. 1687–1694.

Balce, A.E., 1987, Determination of optimum sampling interval in grid digital elevation models (DEM) data acquisition. *Photogrammetric Engineering and Remote Sensing*, **53**(3), pp. 323–330.

BRIESE, C., PFEIFER, N. and DORNINGER, P., 2002, Applications of the robust interpolation method from DTM determination. *International Archives of Photogrammetry and Remote Sensing*, **34**(3A), pp. 55–61.

DANIEL, C. and TENNANT, K., 2001, DEM quality assessment. In *Digital Elevation Models and Applications: The DEM Users Manual*, D.F. Maune (Ed.), pp. 395–440 (Bethesda, MD: ASPRS).

DAVIS, C.H., JIANG, H. and WANG, X., 2001, Modeling and estimation of the spatial variation of elevation error in high resolution DEMs from stereo-image processing. *IEEE Transactions on Geoscience and Remote Sensing*, **39**(11), pp. 2483–2489.

DRAPER, N.R. and SMITH, H., 1981, *Applied regression analysis*, 2nd edition (New York: Wiley).

EVANS, I.S., 1972, General geomorphometry, derivatives of altitude and descriptive statistics. In *Spatial Analysis in Geomorphology*, R.J. Chorley (Ed.), pp. 17–91 (London: Methuen).

FELICÍSIMO, A., 1994, Parametric statistical method for error detection in digital elevation models. *ISPRS Journal of Photogrammetry and Remote Sensing*, **49**(4), pp. 29–33.

FILIN, S. and DOYTSHER, Y., 1998, Estimating accuracy of photogrammetric data. Mechanism and implementation. *Journal of Surveying Engineering*, **124**(4), pp. 156–170.

FISHER, P., 1998, Improved modeling of elevation error with geostatistics. *GeoInformatica*, **2**(3), pp. 215–233.

GAO, J., 1995, Comparison of sampling schemes in constructing DTMs from topographic maps. *ITC Journal*, **1**, pp. 18–22.

GAO, J., 1997, Resolution and accuracy of terrain representation by grid DEMs at a micro-scale. *International Journal of Geographical Information Systems*, **11**(2), pp. 199–212.

GESCH, D., OIMOEN, M., GREENLEE, S., NELSON, C., STEUCK, M. and TYLER, D., 2002, The National Elevation Dataset. *Photogrammetric Engineering and Remote Sensing*, **68**(1), pp. 5–11.

GOLDEN SOFTWARE INC. 2002, *Surfer 8 Users' Guide* (Golden, CO: Golden Software).

GONG, J., LI, Z., ZHU, Q., SUI, H. and ZHOU, Y., 2000, Effects of various factors on the accuracy of DEMs: an intensive experimental investigation. *Photogrammetric Engineering and Remote Sensing*, **66**(9), pp. 1113–1117.

GOODCHILD, M.F. and MARK, D.M., 1987, The fractal nature of geographic phenomena. *Annals of the Association of American Geographers*, **77**(2), pp. 265–278.

GUIBAS, L. and STOLFI, J., 1985, Primitives for the manipulation of general subdivisions and the computation of Voronoi diagrams. *ACM Transactions on Graphics*, **4**(2), pp. 74–123.

HOBSON, R.D., 1972, Surface roughness in topography: quantitative approach. In *Spatial Analysis in Geomorphology*, R.J. Chorley (Ed.), pp. 221–245 (London: Methuen).

HUANG, Y.D., 2000, Evaluation of information loss in digital elevation models with digital photogrammetric systems. *Photogrammetric Record*, **16**(95), pp. 781–791.

KARRAS, G.E., MAVROGENNEAS, N., MAVROMMATI, D. and TSIKONIS, N., 1998, Tests on automatic DEM generation in a digital photogrammetric workstation. *International Archives of Photogrammetry and Remote Sensing*, **32**(2), pp. 136–139.

KUBIK, K. and BOTMAN, A.G., 1976, Interpolation accuracy for topographic and geological surfaces. *ITC Journal*, **2**, pp. 236–274.

LI, Z., 1988, On the measure of digital terrain model accuracy. *Photogrammetric Record*, **12**(72), pp. 873–877.

LI, Z., 1992, Variation of the accuracy of digital terrain models with sampling interval. *Photogrammetric Record*, **14**(79), pp. 113–128.

LI, Z., 1993a, Theoretical models of the accuracy of digital terrain models: an evaluation and some observations. *Photogrammetric Record*, **14**(82), pp. 651–660.

LI, Z., 1993b, Mathematical models of the accuracy of digital terrain model surfaces linearly constructed from square gridded data. *Photogrammetric Record*, **14**(82), pp. 661–674.

López, C., 1997, Locating some types of random errors in digital terrain models. *International Journal of Geographical Information Science*, **11**(7), pp. 677–698.

Makarovic, B., 1972, Information transfer in reconstruction of data from sampled points. *Photogrammetria*, **28**(4), pp. 111–130.

Queija, V.R., Stoker, J.M. and Kosovich, J.J., 2005, Recent US Geological Survey applications of Lidar. *Photogrammetric Engineering and Remote Sensing*, **71**(1), pp. 5–9.

Rees, W.G., 2000, The accuracy of digital elevation models interpolated to higher resolutions. *International Journal of Remote Sensing*, **21**(1), pp. 7–20.

Saleh, R. and Scarpace, F., 2000, Image scanning resolution and surface accuracy; experimental results. *International Archives of Photogrammetry and Remote Sensing*, **33**(part B), pp. 482–485.

Skidmore, A.K., 1989, A comparison of techniques for calculating gradient and aspect from a gridded digital elevation model. *International Journal of Geographical Information Systems*, **3**(4), pp. 323–334.

Smith, S.L., 2004, ISPRS Workshop on 3D reconstruction from laser scanner and InSAR data. *Photogrammetric Record*, **19**(105), pp. 74–76.

Torlegard, K., Ostman, A. and Lindgren, R., 1986, A comparative test of photogrammetrically sampled digital elevation model. *Photogrammetria*, **41**(1), pp. 1–16.

Voltz, M. and Webster, R.A., 1990, A comparison of kriging cubic splines and classification for predicting soil properties from sample information. *Journal of Soil Science*, **41**(3), pp. 473–490.

Wang, L., 1990, *Comparative studies of spatial interpolation accuracy*, Master thesis, Department of Geography, University of Georgia, USA.

Weng, Q., 2002, Quantifying uncertainty of digital elevation models derived from topographic maps. In *Advances in Spatial Data Handling*, D. Richardson and P. van Oosterom (Eds), pp. 403–418 (New York: Springer).

Wood, J.D., 1996, The geomorphological characterisation of digital elevation models. PhD thesis, University of Leicester, UK.

Wood, J.D. and Fisher, P.F., 1993, Assessing interpolation accuracy in elevation models. *IEEE Computer Graphics & Applications*, **13**(2), pp. 48–56.

Yang, X. and Hodler, T., 2000, Visual and statistical comparisons of surface modelling techniques for point-based environmental data. *Cartography and Geographic Information Science*, **27**(2), pp. 165–175.